

QUARK-GLUON STRING MODEL DESCRIPTION OF BARYON PRODUCTION IN $K^\pm N$ INTERACTIONS

G. H. Arakelyan¹, C. Merino², and Yu. M. Shabelski³

ABSTRACT

The process of baryon production in Kp collisions at high energies is considered in the framework of the Quark-Gluon String Model. The contribution of the string-junction mechanism to the strange baryon production is analysed. The results of numerical calculations are in reasonable agreement with the data on inclusive spectra of p , Λ , $\bar{\Lambda}$, and on the $\bar{\Lambda}/\Lambda$ asymmetry. The predictions for Ξ and Ω baryons are presented.

¹Permanent address: Yerevan Physics Institute, Armenia
E-mail: argev@mail.yerphi.am

²Permanent address: Departamento de Física de Partículas, Facultade de Física, and Instituto Galego de Altas Enerxías (IGAE), Universidade de Santiago de Compostela, Galicia, Spain
E-mail: merino@fpaxpl.usc.es

³Permanent address: Petersburg Nuclear Physics Institute, Gatchina, St.Petersburg, Russia
E-mail: shabelsk@thd.pnpi.spb.ru

1. INTRODUCTION

The Quark–Gluon String Model (QGSM) is based on the Dual Topological Unitarization (DTU) and it describes quite reasonably and in a theoretically consistent way many features of high energy production processes, including the inclusive spectra of different secondary hadrons, their multiplicities, etc., both in hadron-nucleon and hadron-nucleus collisions [1]-[6]. High energy interactions are considered as taking place via the exchange of one or several Pomerons, and all elastic and inelastic processes result from cutting through or between those exchanged Pomerons [7, 8]. The possibility of different numbers of Pomerons to be exchanged introduces absorptive corrections to the cross-sections which are in agreement with the experimental data on production of hadrons consisting of light quarks. Inclusive spectra of hadrons are related to the corresponding fragmentation functions of quarks and diquarks, which are constructed in terms of the intercepts of well known Regge trajectories [9].

In papers [10]-[13] the processes connected with the transfer of baryon charge over long rapidity distances were discussed. In the string models baryons are considered as configurations consisting of three strings attached to three valence quarks and connected in one point that it is called string junction (SJ) [14, 15, 16]. Thus the SJ mechanism has a nonperturbative origin in QCD.

It is very important to understand the role of the SJ mechanism in the dynamics of high-energy hadronic interactions, in particular in processes implying baryon number transfer [17]-[24]. Significant results on this question were obtained in [10, 11, 13, 24]. In these papers the SJ mechanism was used to analyse the strange baryon production in πp and pp interactions.

The present paper is devoted to the calculation of inclusive spectra of fast baryon production in the case of kaon beam and to the analysis of the contribution of SJ mechanism in Kp collisions.

The strange quark in the kaon carries, on the average, a larger fraction of the momentum than the non-strange quark. This translates in a harder spectra for the secondary particles produced as result of the fragmentation of the strange quark. How much harder these spectra become it will depend on the interaction mechanism, and therefore the comparison of the theoretical calculations with experiment offers the possibility of making a more complete test of the model. The first consideration of the spectra of Λ -baryon production on kaon beam [25, 26] was made in [6], where strange baryon production was considered in the QGSM scheme without taking into account the SJ contribution.

In the present paper we analyse the existing data on spectra and asymmetry of Λ and $\bar{\Lambda}$ production on K -beams [25]-[30]. We use the same parametrisations of diquark fragmentation functions to strange baryons and the same Regge trajectory intercepts as in [10, 11].

The obtained description of the experimental data is presented and new information on the properties of the SJ dynamics is extracted.

In this paper we mainly compare the experimental data with the result of our calculations for SJ intercept $\alpha_{SJ} = 0.9$.

2. INCLUSIVE SPECTRA OF SECONDARY HADRONS IN Kp COLLISIONS

As it is thoroughly known the exchange of one or several Pomerons is one basic feature of high energy hadron-nucleon and hadron-nucleus interactions in the frame of QGSM and Dual Parton Model (DPM). Each Pomeron corresponds to a cylindrical diagram, and thus when cutting a Pomeron two showers of secondaries are produced. The inclusive spectrum of secondaries is determined by the convolution of diquark, valence, and sea quark distribution functions in the incident particle, $u(x, n)$, and the fragmentation functions of quarks and diquarks into secondary hadrons, $G(z)$.

The inclusive spectrum (i.e. Feynman- x distribution) of a secondary hadron h is determined in QGSM by the expression [1]

$$\frac{x_E}{\sigma_{inel}} \cdot \frac{d\sigma}{dx_F} = \sum_{n=1}^{\infty} w_n \cdot \varphi_n^h(x_F), \quad (1)$$

where $x_E = E/E_{max}$, and

$$w_n = \sigma_n / \sum_{n=1}^{\infty} \sigma_n \quad (2)$$

is the weight of the diagram with n cutted Pomerons. The n cutted Pomeron cross-sections σ_n are calculated using the quasi-eikonal approximation with a supercritical Pomeron [8]:

$$\sigma_n = \frac{\sigma_P}{n \cdot z} \cdot \left(1 - e^{-z} \sum_{k=0}^{\infty} \frac{z^k}{k!} \right), \quad n \geq 1, \quad (3)$$

$$z = \frac{2C_P \gamma_P}{R_P^2 + \alpha'_P \ln(s/s_0)} \cdot \left(\frac{s}{s_0} \right)^\Delta, \quad (4)$$

$$\sigma_P = 8\pi \gamma_P \cdot \left(\frac{s}{s_0} \right)^\Delta, \quad (5)$$

where σ_P is the Pomeron contribution to the total cross-section, $\Delta = \alpha_P(0) - 1$ is the excess of the Pomeron intercept over 1 (supercritical Pomeron), and parameters γ_P , R_P^2 , and C_P take the values for the case of Kp interactions presented in [31] (see also [6]).

The function $\varphi_n^h(x_F)$ in Eq. (1) determines the contribution of the diagram in which n Pomerons are cut. In the case of Kp collisions this function has the form [6]:

$$\varphi_n^{Kp \rightarrow h}(x_F) = f_q^h(x_+, n) \cdot f_q^h(x_-, n) + f_q^h(x_+, n) \cdot f_{qq}^h(x_-, n) + 2(n-1) f_s^h(x_+, n) \cdot f_s^h(x_-, n), \quad (6)$$

with

$$x_{\pm} = \frac{1}{2} \left[\left(\frac{4m_{\pm}^2}{s} + x_F^2 \right)^{\frac{1}{2}} \pm x_F \right]. \quad (7)$$

The quantities f_{qq} , f_q , $f_{\bar{q}}$, and f_s in Eq. (6) correspond to the contributions of the diquark, the valence quark and antiquark, and the sea quarks, while the contributions of the incident particle and the target proton depend on the variables x_+ and x_- , respectively.

The values of $f_{qq}^h(x_{\pm}, n)$, $f_q^h(x_{\pm}, n)$, $f_{\bar{q}}^h(x_{\pm}, n)$, and $f_s^h(x_{\pm}, n)$ can be obtained through the convolution of the corresponding momentum distribution of the diquarks, valence quarks, and sea quarks in the colliding hadrons, $u(x)$, and the function for fragmentation $G^h(z)$ of either diquarks or quarks into secondary hadrons:

$$f_q^h(x_{\pm}, n) = \int_{x_{\pm}}^1 u_q(x_1, n) \cdot G_q^h(x_{\pm}/x_1) dx_1, \quad (8)$$

$$f_{qq}^h(x_-, n) = \frac{2}{3} \int_{x_-}^1 u_{ud}(x_1, n) \cdot G_{ud}^h(x_-/x_1) dx_1 + \frac{1}{3} \int_{x_-}^1 u_{uu}(x_1, n) \cdot G_{uu}^h(x_-/x_1) dx_1 \quad (9)$$

$$\begin{aligned} f_s^h(x_{\pm}, n) &= \frac{1}{2 + \delta} \left[\int_{x_{\pm}}^1 u_{\bar{u}}(x_1, n) \frac{G_{\bar{u}}^h(x_{\pm}/x_1) + G_u^h(x_{\pm}/x_1)}{2} dx_1 \right. \\ &+ \int_{x_{\pm}}^1 u_{\bar{d}}(x_1, n) \frac{G_{\bar{d}}^h(x_{\pm}/x_1) + G_d^h(x_{\pm}/x_1)}{2} dx_1 \\ &\left. + \delta \cdot \int_{x_{\pm}}^1 u_{\bar{s}}(x_1, n) \frac{G_{\bar{s}}^h(x_{\pm}/x_1) + G_s^h(x_{\pm}/x_1)}{2} dx_1 \right]. \quad (10) \end{aligned}$$

The parameter $\delta \sim 0.2-0.3$ determines here the relative suppression of strange quarks in the sea. It is important to note that we use the factor δ in two cases. The first one is presented in Eq. (10), where its variation from 0.2 to 0.3 changes the model predictions very little. The second case is discussed in the Appendix, where δ determines the relative ratio of strange and non-strange baryon production. In the latter case the variation of δ from 0.2 to 0.32 changes the model predictions rather significantly, as it is shown in the next section.

The detailed description of high energy hadron-nucleon cross-sections on the base of the Reggeon calculus has been presented in many papers (see, for instance, [1, 3, 4, 5, 6]).

The diquark and quark distribution functions and the fragmentation functions are determined by the Regge intercepts [9].

The complete set of distribution and fragmentation functions used in this paper is presented in the Appendix.

As it was shown in [10] the net baryon charge can be obtained from the fragmentation of the diquark giving rise to a leading baryon.

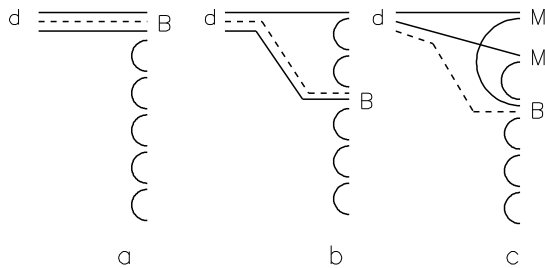


Figure 1: QGSM diagrams describing secondary baryon B production by diquark d : (a) initial SJ together with two valence quarks and one sea quark, (b) initial SJ together with one valence quark and two sea quarks, and (c) initial SJ together with three sea quarks.

To produce a secondary baryon in the process of diquark fragmentation there exist three possibilities that are shown in Fig. 1. Thus the secondary baryon can consist of: the initial SJ together with two valence and one sea quarks (Fig. 1a), the initial SJ together with one valence and two sea quarks (Fig. 1b), the initial SJ together with three sea quarks (Fig. 1c). The fraction of the incident baryon energy carried by the secondary baryon decreases from case (a) to case (c), whereas the mean rapidity gap between the incident and secondary baryon increases.

The diagram of Fig. 1b has been used for the description of baryon number transfer in QGSM [1, 19]. Also it describes also the fast meson production by a diquark [9].

In this paper we mainly analyse the contribution of the graph in Fig. 1c to the diquark fragmentation function. This contribution has been determined for kaon induced reactions in the forward hemisphere in [10]. Its magnitude is proportional to one coefficient that it will be denoted by ε (the suppression factor of the process of Fig. 1c compared to those of the processes in Figs. 1a and 1b, see the Appendix), and that it was firstly analysed in [10, 11, 13] for the case of proton and pion induced reactions.

The SJ mechanism has a nonperturbative origin and since it is at present not possible to determine α_{SJ} in QCD from first principles. Thus we treat α_{SJ} and ε as phenomenological parameters which should be determined from experimental data. In the present calculation, we use the values of parameter $\alpha_{SJ} = 0.9$ and $\varepsilon = 0.024$, as it was done in [11, 12].

3. RESULTS AND COMPARISON WITH EXPERIMENT

In this paper we mainly consider the existing experimental data on Λ and $\bar{\Lambda}$ production on nucleon target [25]-[30]. We present the comparison of QGSM calculations with the experimental data on spectra and on asymmetry of Λ and $\bar{\Lambda}$ hyperons. We also analyse the role of the strange quark suppression factor δ (see the Appendix), and we present

results of the calculations for two values of this parameter. As it was shown in [12], the better agreement of QGSM with data on strange baryon production on nucleus was obtained with $\delta = 0.32$, instead of the previous value $\delta = 0.2$. In principal we cannot exclude the possibility that the value of δ could be different for secondary baryons and for mesons (i.e., for Λ -baryon and for kaon).

The fragmentation functions into $\bar{\Lambda}$ do not depend on the SJ mechanism, so the $\bar{\Lambda}$ spectra are the same for different values of α_{SJ} , and also they have a very small dependence on the strange quark suppression factor δ since they depend on δ only via Eq. (10).

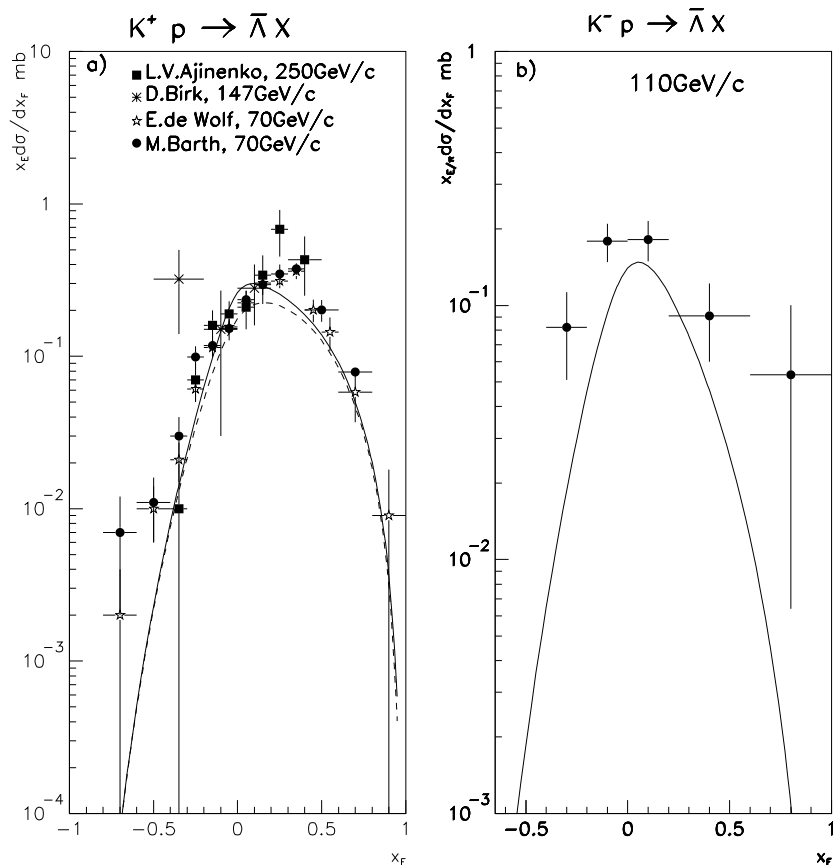


Figure 2: The QGSM description of x_F spectra of $\bar{\Lambda}$ in: (a) K^+p collisions at 70 GeV/c [28, 26], 147 GeV/c [30], and 250 GeV/c [29]. The solid curve corresponds to 250 GeV/c and the dashed curve to 70 GeV/c. (b) K^-p collisions at 110 GeV/c [25]. The curve shows to the QGSM prediction.

The inclusive spectra of $\bar{\Lambda}$ produced in K^+p collisions at $E_{lab} = 250$ GeV/c [29], 147 GeV/c [30], and 70 GeV/c [28, 26] are shown in Fig. 2a. The corresponding spectrum

of $\bar{\Lambda}$ produced in K^-p collisions at $E_{lab} = 110$ GeV/c is shown in Fig. 2b. The two curves on Fig. 2a correspond to two different values of E_{lab} (the solid curve stands for $E_{lab} = 250$ GeV/c and the dashed curve for $E_{lab} = 70$ GeV/c). As we see there is only very small difference between these two curves in the central region, so the curve for $E_{lab} = 147$ GeV/c, which lies in between the other two, is not presented.

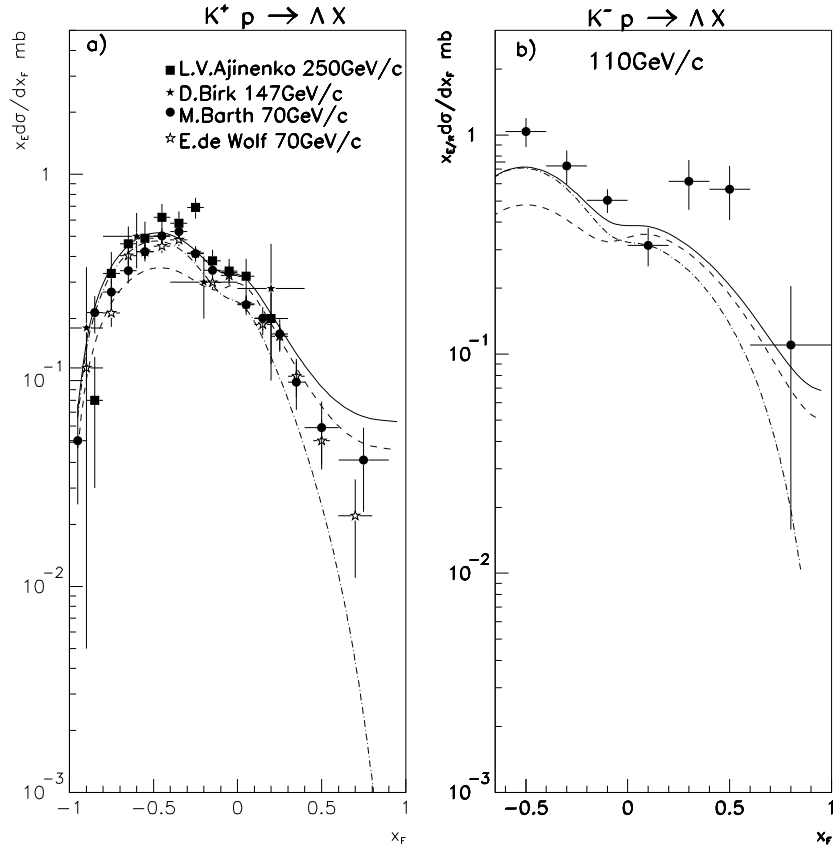


Figure 3: The QGSM description of x_F spectra of Λ in: (a) K^+p collisions at 70 GeV/c [28, 26], 147 GeV/c [30], and 250 GeV/c [29]. (b) K^-p collisions at 110 GeV/c [25]. The solid curves correspond to $\alpha_{SJ} = 0.9$, $\varepsilon = 0.024$, and $\delta = 0.32$, the dashed curves to $\delta = 0.2$, and the dashed-dotted curves to $\varepsilon = 0$.

The inclusive spectra of Λ produced in K^+p collisions at $E_{lab} = 250$ GeV/c [29], 147 GeV/c [30], and 70 GeV/c [28, 26] are shown in Fig. 3a. The corresponding spectra of Λ produced in K^-p collisions at $E_{lab} = 110$ GeV/c [25] are shown on Fig. 3b.

In the following figures the solid curves will correspond to calculations with $\alpha_{SJ} = 0.9$, $\varepsilon = 0.024$, and $\delta = 0.32$, the dashed curves to $\alpha_{SJ} = 0.9$, $\varepsilon = 0.024$, and $\delta = 0.2$,

and the dashed-dotted curves will stand for calculations with $\varepsilon = 0$ (i.e., without SJ contribution). In general it seems that the solid curves are in slightly better agreement with the data, although the difference between the different curves is not large in the region where experimental data exist.

In Fig. 4 we show the comparison of the QGSM calculations with the data on the $\bar{\Lambda}/\Lambda$ asymmetry produced in K^+p (Fig. 4a) and K^-p (Fig. 4b) interactions at 250 GeV/c [27]. The $\bar{\Lambda}/\Lambda$ asymmetry is defined as

$$A(\bar{\Lambda}/\Lambda) = \frac{N_\Lambda - N_{\bar{\Lambda}}}{N_\Lambda + N_{\bar{\Lambda}}} \quad (11)$$

for each x_F bin.

The asymmetry data are rather interesting. In the proton fragmentation region the values of $A(\bar{\Lambda}/\Lambda)$ are close to unity, and that is natural since a proton fragments into Λ with significantly larger probability than into $\bar{\Lambda}$. In the kaon fragmentation region (at x_F values where experimental data exist) $A(\bar{\Lambda}/\Lambda)$ becomes negative and decreases very fast in the case of K^+ beam. In the case of K^- beam it increases very fast with x_F and the difference between the calculations with different parameters is rather small. Both these behaviors are also natural, because the K^+ contains a \bar{s} valence quark which preferably fragments into $\bar{\Lambda}$, while the valence s quark from the K^- fragments rather often into Λ . However, in both cases the $A(\bar{\Lambda}/\Lambda)$ experimental x_F -dependences are much steeper than the theoretical predictions. This is a probable indication that the fragmentation functions $s \rightarrow \Lambda$ and $\bar{s} \rightarrow \bar{\Lambda}$ should be further enhanced.

In the K^+ fragmentation region (Fig. 4a) the predicted values of $A(\bar{\Lambda}/\Lambda)$ at $x_F > 0.4$ show a change of behavior and they start increasing. In this region the contribution of the direct fragmentation of $\bar{s} \rightarrow \bar{\Lambda}$, which makes $A(\bar{\Lambda}/\Lambda)$ to decrease, becomes smaller than the effect of SJ diffusion which increases the multiplicity of Λ . The measurement of the asymmetry $A(\bar{\Lambda}/\Lambda)$ in the region $x_F \geq 0.4$ in K^+p collisions could make the situation more clear.

The inclusive spectra of secondary protons produced in K^+p collisions at energies $E_{lab} = 250$ GeV/c [29], together with the theoretical curves, are presented in Fig. 5. Unfortunately the data on proton production on K beams were only measured in the backward hemisphere where they are practically the same that in the case of the pp interaction, with the evident difference in normalization.

In Figs. 6 and 7 we present the predictions for cross sections (Fig. 6) and asymmetries (Fig. 7) for Ξ^- and Ω production in K^+p and K^-p collisions at 250 GeV/c. In the central region of K^+p collisions the yields of Ξ^- and $\bar{\Xi}^+$, as well as of Ω^- and $\bar{\Omega}^+$ are predicted to be practically the same. The smaller fragmentation function of valence \bar{s} quark into strange baryon is compensated by the larger fragmentation function of the target diquark.

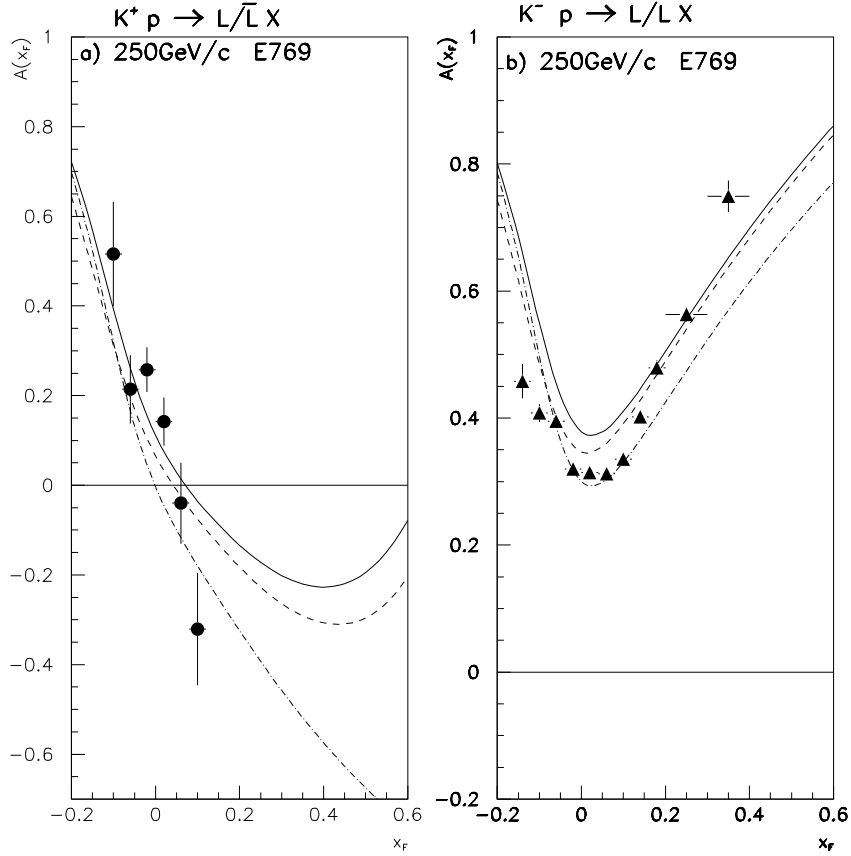


Figure 4: The $\bar{\Lambda}/\Lambda$ asymmetry in (a) K^+p and (b) K^-p collisions. Experimental data at 250 GeV/c [27] and the corresponding QGSM description. The solid curve corresponds to $\alpha_{SJ} = 0.9$, $\varepsilon = 0.024$, and $\delta = 0.32$, the dashed curve to $\delta = 0.2$, and the dashed-dotted curve to $\varepsilon = 0$.

The large difference between Ω and $\bar{\Omega}$ production cross-sections in K^-p collisions (Fig. 6b) can be explained by the presence of valence s quark in K^- meson directly fragmenting to Ω baryon, and by absence of valence quarks for the case of $\bar{\Omega}$ production. For Ξ^- and $\bar{\Xi}^+$ production one also has valence s quark going into the leading Ξ^- baryon. So, as it can be seen in Fig. 6b, the cross-sections for Ξ^- and Ω are larger than the corresponding cross-sections for antibaryons.

In K^+p collisions one has the valence \bar{s} quark to produce leading $\bar{\Xi}^+$ and $\bar{\Omega}$. Thus up to $x \sim 0.5$, these cross sections are larger than those for producing Ξ^- and Ω . At larger x_F ($x_F \rightarrow 1$) the antibaryons cross-sections fall more rapidly.

The predictions for asymmetry in Ξ and Ω baryon production in K^+p and K^-p interactions are presented in Fig. 7. Here the general situation is similar to that of

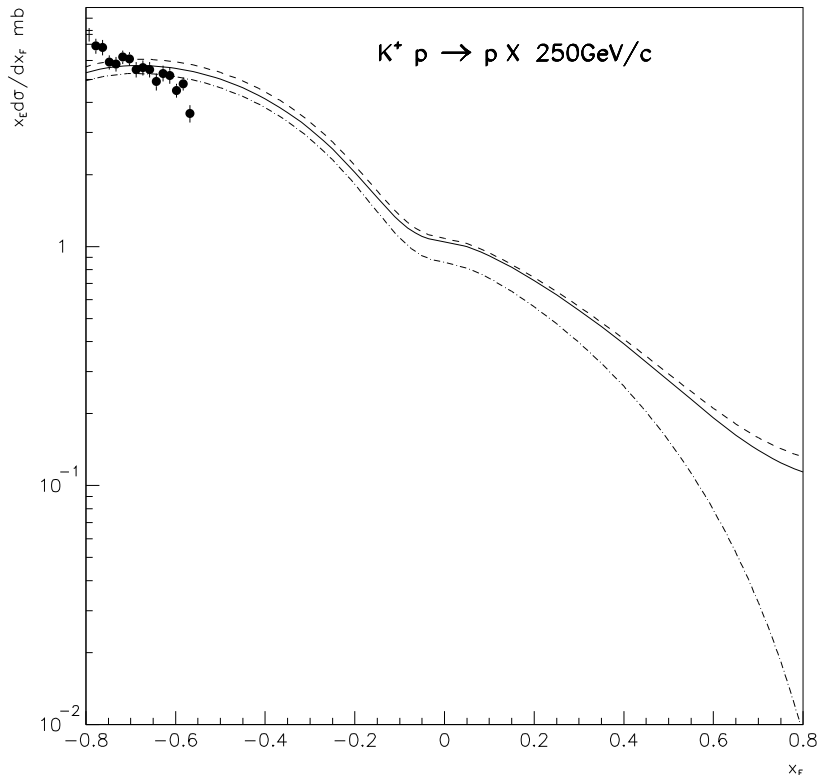


Figure 5: The x_F -dependence of the spectra of protons in K^+p collisions. Experimental data at 250 GeV/c [29] and the corresponding QGSM description. The full line corresponds to $\alpha_{SJ} = 0.9$, $\varepsilon = 0.024$, and $\delta = 0.32$, the dashed line to $\delta = 0.2$, and the dashed-dotted line to $\varepsilon = 0$.

the case of asymmetry in Λ production shown in Fig. 4. In the case of K^- beam the asymmetry for both Ξ and Ω productions increases in the whole region of positive x_F .

5. CONCLUSIONS

It is shown that the experimental data can not discriminate among the different sets of parameters in the model. The results of the calculations with the value $\alpha_{SJ} = 0.5$ do not differ from the results with $\alpha_{SJ} = 0.9$ in any significant way. Even the value $\varepsilon = 0$ seems compatible with the data. For K^+ beam all curves show a more or less reasonable agreement with experimental data on cross-sections and asymmetry (Figs. 2a and 3a).

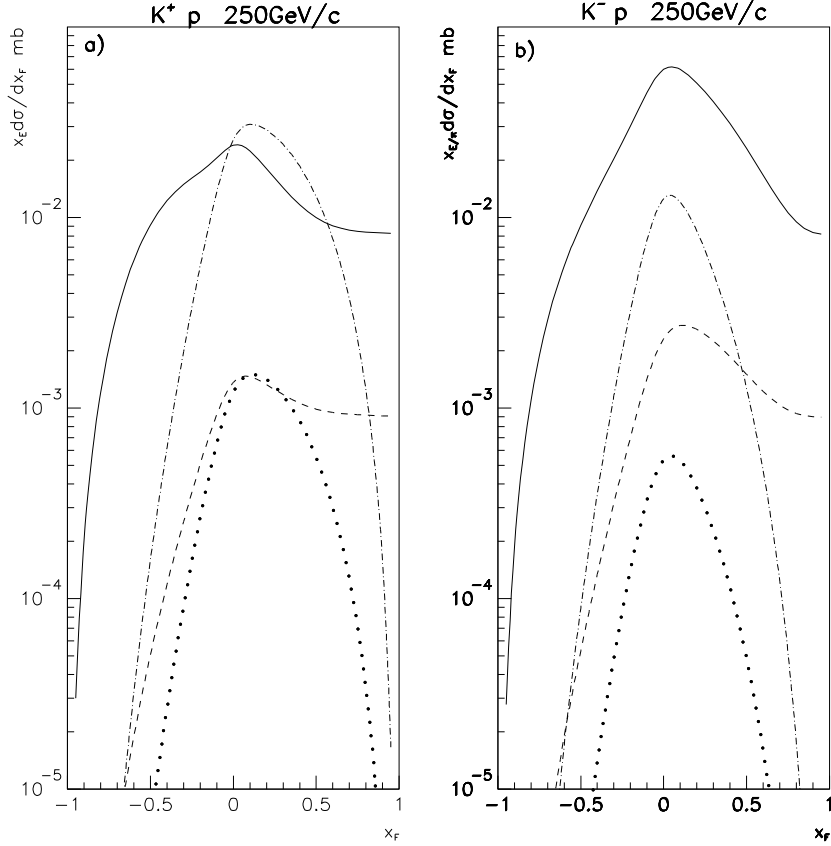


Figure 6: QGSM prediction for the x_F -dependence of the spectra of heavy strange baryons in (a) K^+p and (b) K^-p collisions at 250 GeV/c. Solid curves are for Ξ^- , dash-dotted curves for Ξ^+ , dashed curves for Ω^- , and dotted curves for $\bar{\Omega}^+$.

The difference between the results for the two values of the strangeness suppression factor δ is small in the backward hemisphere but it appears evident when x_F is positive both for cross-sections and asymmetries. Unfortunately, the data on asymmetry are concentrated in the central region $-0.2 < x_F < 0.1$ where the difference among curves is not so large.

The situation for K^- beam seems worse than in the K^+ case since all curves are, as a rule, below the experimental data. Both the number and the quality of experimental data on K^- beam are not high enough.

One has also to note that the QGSM does not reproduce the experimentally observed maximum in the Λ spectrum in the range $x_F = 0.2 - 0.4$ which is seen in Fig. 3b (there are no analogous maxima in the reactions $\pi^-p \rightarrow \bar{p}X$ and $\pi^+p \rightarrow pX$ [32]).

QGSM predicts a weak energy dependence of the Λ and $\bar{\Lambda}$ production cross-section in Kp collisions at the considered energies.

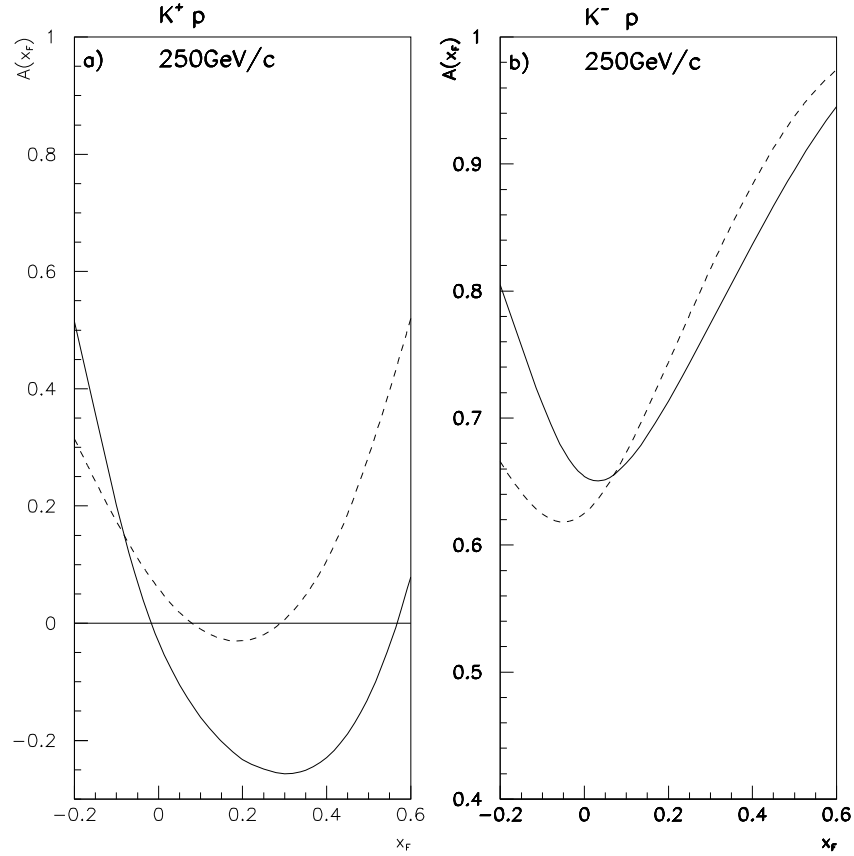


Figure 7: QGSM prediction for the x_F -dependence of the asymmetry of heavy strange baryons in (a) K^+p and (b) K^-p collisions at 250 GeV/c. Solid curves are for Ξ^- , dashed curves for Ω^-

Finally, the experimental data on high-energy Λ production are not in contradiction with the possibility of baryon charge transfer over large rapidity distances. The $\bar{\Lambda}/\Lambda$ asymmetry is provided by SJ diffusion through baryon charge transfer.

The presence of baryon asymmetry in the projectile hemisphere for Kp collisions provides good evidence for such a mechanism.

To get a good understanding of the dynamics of the baryon charge transfer over large rapidity distances new experimental data in meson and baryon collisions with nucleons and nuclear targets are needed.

Acknowledgments

The authors are thankful to A.B. Kaidalov and C. Pajares for useful discussions.

This work was partially financed by CICYT of Spain through contract FPA2002-01161, and by Xunta de Galicia through contract PGIDIT03PXIC20612PN.

G. H. Arakelyan and C. Merino were also supported by NATO grant CLG.980335 and Yu. M. Shabelski by grants NATO PDD (CP) PST.CLG 980287, RCGSS-1124.2003.2. G.H.A. thanks the Xunta de Galicia for financial support.

G.H.A and Yu.M.Sh. want to thank the members of the Department of Particles Physics and of the Instituto Galego de Altas Enerxías (IGAE), University of Santiago de Compostela, Galicia, Spain, for their kind hospitality during the final stage of this work.

APPENDIX: QUARK AND DIQUARK DISTRIBUTIONS AND THEIR FRAGMENTATION FUNCTIONS

The distribution functions of the valence quarks (u quark for K^+ and s quark for K^-) in the K meson were chosen in the form [6]:

$$\begin{aligned} u_s^{K^-}(x, n) &= u_s^{K^+}(x, n) = C_q x^{-\alpha_\varphi} (1-x)^{-\alpha_R+n-1}, \\ u_{\bar{u}}^{K^-}(x, n) &= u_u^{K^+}(x, n) = C_{\bar{q}} x^{-\alpha_R} (1-x)^{-\alpha_\varphi+n-1}, \end{aligned} \quad (12)$$

for valence quarks, and

$$u(x, n) = C x^{-\alpha_R} (1-x)^{n-\alpha_R-1} [1 - \delta \sqrt{1-x}], \quad n > 1, \quad (13)$$

$$u_s(x, n) = C_s x^{-\alpha_R} (1-x)^{n-1}, \quad n > 1, \quad (14)$$

for sea quarks.

The strange valence quark in the K^- meson (and the strange valence antiquark in the K^+ meson) carries on the average twice as much momentum as the nonstrange antiquark.

The δ is the relative probability to find a strange quark in the sea, while the normalization factors C_i are determined by the condition

$$\int_0^1 u_i(x, n) dx = 1, \quad (15)$$

and the sum rule

$$\int_0^1 \sum_i u_i(x, n) x dx = 1 \quad (16)$$

is fulfilled.

The quark and diquark distribution functions in the proton have been taken as in [10].

The fragmentation functions of quarks and diquarks have been slightly changed with respect to Refs. [4, 5] in order to obtain a better agreement with the existing experimental data (the fragmentation functions in [4, 5] correspond to $\varepsilon = 0$). We have used the following functional form for the quark fragmentation functions:

$$G_u^p = G_d^p = a_{\bar{N}} (1-z)^{\lambda+\alpha_R-2\alpha_B} \cdot (1+a_1 z^2), \quad G_u^{\bar{p}} = G_d^{\bar{p}} = (1-z) \cdot G_u^p, \quad (17)$$

$$G_u^\Lambda = G_d^\Lambda = a_{\bar{\Lambda}} (1-z)^{\lambda+\alpha_R-2\alpha_B+\Delta\alpha} \cdot (1+a_1 z^2), \quad G_u^{\bar{\Lambda}} = G_d^{\bar{\Lambda}} = (1-z) \cdot G_u^\Lambda, \quad (18)$$

$$G_d^{\Xi^-} = \frac{a_{\bar{\Xi}}}{a_{\bar{\Lambda}}} (1-z)^{\Delta\alpha} G_u^\Lambda, \quad G_u^{\Xi^-} = G_u^{\bar{\Xi}} = (1-z) G_d^{\Xi^-}, \quad (19)$$

$$G_u^\Omega = G_d^\Omega = G_u^{\bar{\Omega}} = G_d^{\bar{\Omega}} = \frac{a_{\bar{\Omega}}}{a_{\bar{\Xi}}} (1-z)^{\Delta\alpha} G_u^{\Xi^-}, \quad (20)$$

$$G_s^p(z) = a_N (1-z)^{\lambda+\alpha_R-2\alpha_B+1.5} \cdot (1+a_1 z), \quad (21)$$

$$G_s^{\bar{p}}(z) = a_{\bar{N}}(1-z)^{\lambda+\alpha_R-2\alpha_B+0.5} \cdot (1+a_1z) , \quad (22)$$

$$G_s^{\Lambda}(z) = a_{\bar{N}}(1-z)^{\lambda+\alpha_R-2\alpha_B} \cdot (1+a_1z) , \quad (23)$$

$$G_s^{\bar{\Lambda}}(z) = a_{\bar{\Lambda}}(1-z)^{\lambda+\alpha_R-2\alpha_B+2(1-\alpha_R)+2\Delta\alpha} , \quad (24)$$

$$G_s^{\Xi^-}(z) = a_{\bar{\Lambda}}(1-z)^{\lambda+\alpha_R-2\alpha_B+\Delta\alpha} \cdot (1+a_1z) , \quad (25)$$

$$G_s^{\Xi^-}(z) = a_{\Xi^-}(1-z)^{\lambda+\alpha_R-2\alpha_B+\Delta\alpha+2(\alpha_R-\alpha_\phi)} \cdot (1+a_1z) , \quad (26)$$

$$G_s^{\bar{\Omega}}(z) = a_{\bar{\Omega}}(1-z)^{4\lambda+\alpha_R-2\alpha_B+1} \cdot (1+a_1z) , \text{ and} \quad (27)$$

$$G_s^{\Omega}(z) = a_{\Xi^-}(1-z)^{3\lambda+\alpha_R-2\alpha_B} \cdot (1+a_1z) , \quad (28)$$

with

$$\alpha_R = 0.5, \alpha_\Phi = 0, \alpha_B = -0.5, \Delta\alpha = \alpha_R - \alpha_\phi, \lambda = 2\alpha' \cdot \langle p_t^2 \rangle = 0.5 . \quad (29)$$

The fragmentation function of s quark into Λ in Eq. 23 differs from the one in [6]. We propose that the fragmentation functions of strange s quark and light u quark into Λ describe the same mechanism: in both cases the fragmented quark captures the ud diquark with the corresponding coefficient being the same, $a_{\bar{N}}$. For the fragmentation of s quark into $\bar{\Lambda}$ we should change the strange quark by the strange antiquark so the exchange of one $s\bar{s}$ system occurs.

The parametrisation of diquark fragmentation functions taking into account the SJ contribution was analysed in previous papers [10, 11, 13], in which two values of the SJ intercept $\alpha_{SJ} = 0.5$ and $\alpha_{SJ} = 0.9$ [13] were considered. In the present paper we have used the parametrisations of fragmentation functions of diquarks into strange baryons for $\alpha_{SJ} = 0.9$ and the corresponding set of parameters, as it has been done in [11, 12]. These rather large value of α_{SJ} is confirmed by high energy data from HERA and RHIC [11].

Diquark fragmentation functions have more complicated forms. They contain two contributions. The first one corresponds to the central production of a $B\bar{B}$ pair and it can be described by the formulas:

$$G_{uu}^p = G_{ud}^p = G_{uu}^{\bar{p}} = G_{ud}^{\bar{p}} = a_{\bar{N}}(1-z)^{\lambda-\alpha_R+4(1-\alpha_B)} , \quad (30)$$

$$G_{uu}^\Lambda = G_{ud}^\Lambda = G_{uu}^{\bar{\Lambda}} = G_{ud}^{\bar{\Lambda}} = a_{\bar{\Lambda}}(1-z)^{\Delta\alpha} G_{uu}^p , \quad (31)$$

$$G_{uu}^{\Xi^-} = G_{ud}^{\Xi^-} = G_{uu}^{\Xi^-} = G_{ud}^{\Xi^-} = a_{\Xi^-}(1-z)^{\Delta\alpha} G_{uu}^\Lambda , \text{ and} \quad (32)$$

$$G_{uu}^\Omega = G_{ud}^\Omega = G_{uu}^{\bar{\Omega}} = G_{ud}^{\bar{\Omega}} = a_{\bar{\Omega}}(1-z)^{\Delta\alpha} G_{uu}^{\Xi^-} , \quad (33)$$

with the same $\Delta\alpha$ as in Eq. (29).

The second contribution is connected with the direct fragmentation of the initial baryon into the secondary one with conservation of SJ . As it was discussed above, there exist three different types of such contributions (Figs. 1a-1c). These contributions are

determined by expressions similar to Eqs. (8- 10) with the corresponding fragmentation functions given by

$$G_{uu}^p = G_{ud}^p = a_N z^\beta \left[v_0 \varepsilon (1-z)^2 + v_q z^{2-\beta} (1-z) + v_{qq} z^{2.5-\beta} \right], \quad (34)$$

$$G_{ud}^\Lambda = a_N z^\beta \left[v_0 \varepsilon (1-z)^2 + v_q z^{2-\beta} (1-z) + v_{qq} z^{2.5-\beta} \right] (1-z)^{\Delta\alpha}, \quad G_{uu}^\Lambda = (1-z) G_{ud}^\Lambda, \quad (35)$$

$$G_{d,SJ}^{\Xi^-} = a_N z^\beta \left[v_0 \varepsilon (1-z)^2 + v_q z^{3/2} (1-z) \right] (1-z)^{2\Delta\alpha}, \quad G_{u,SJ}^{\Xi^-} = (1-z) G_{d,SJ}^{\Xi^-}, \quad (36)$$

$$G_{SJ}^\Omega = a_N v_0 \varepsilon z^\beta (1-z)^{2+3\Delta\alpha}, \quad (37)$$

with $\beta = 1 - \alpha_{SJ}$. As for the factor $z^\beta \cdot z^{2-\beta}$ in the second term, it is $2(\alpha_R - \alpha_B)$ [1]. For the third term we have added an extra factor $z^{1/2}$.

The probabilities of transition into the secondary baryon of SJ without valence quarks, I_3 , SJ plus one valence quark, I_2 , and SJ plus a valence diquark, I_1 , are taken from the simplest quark combinatorials [23]. Assuming that the strange quark suppression is the same in all these cases, we obtain for the relative yields of different baryons from SJ fragmentation without valence quarks:

$$I_3 = 4L^3 : 4L^3 : 12L^2S : 3LS^2 : 3LS^2 : S^3, \quad (38)$$

for secondary p , n , $\Lambda + \Sigma$, Ξ^0 , Ξ^- , and Ω , respectively.

For I_2 we obtain

$$I_{2u} = 3L^2 : L^2 : 4LS : S^2 : 0, \quad (39)$$

and

$$I_{2d} = L^2 : 3L^2 : 4LS : 0 : S^2 \quad (40)$$

for secondary p , n , $\Lambda + \Sigma$, Ξ^0 and Ξ^- .

For I_1 we have

$$I_{1uu} = 2L : 0 : S \quad (41)$$

and

$$I_{1ud} = L : L : S \quad (42)$$

for secondary p , n , and $\Lambda + \Sigma$. The ratio $\delta = S/L$ determines the strange suppression factor, and $2L + S = 1$. In the numerical calculations we have compared the results for two different values $\delta = 0.2$ and $\delta = 0.32$.

In agreement with the empirical rule we assume that $\Sigma^+ + \Sigma^- = 0.6\Lambda$ [33] in Eqs. (38)-(40). As it is customary Σ^0 are included into Λ . Note that this empirical rule, used in many experimental papers, is not consistent with the simplest quark statistics rules [34].

The values of v_0 , v_q , and v_{qq} are directly determined by the corresponding coefficients in Eqs. (38)-(42), together with the probabilities to fragment a qqs system into $\Sigma^+ + \Sigma^-$

and into Λ , given above. Thus we have:
for incident uu diquark and secondary proton

$$v_0 = 4L^3, v_q = 3L^2, v_{qq} = 2L, \quad (43)$$

for incident ud diquark and secondary proton

$$v_0 = 4L^3, v_q = 2L^2, v_{qq} = L, \quad (44)$$

for incident uu diquark and secondary Λ

$$v_0 = \frac{12}{1.6}SL^2, v_q = \frac{4}{1.6}SL, v_{qq} = \frac{1}{4}S, \quad (45)$$

for incident ud diquark and secondary Λ

$$v_0 = \frac{12}{1.6}SL^2, v_q = \frac{4}{1.6}SL, v_{qq} = S, \quad (46)$$

for incident u quark and secondary Ξ^-

$$v_0 = 3S^2L, v_q = 0, \quad (47)$$

for incident d quark and secondary Ξ^-

$$v_0 = 3S^2L, v_q = S^2, \quad (48)$$

and for incident SJ and secondary Ω^-

$$v_0 = S^3. \quad (49)$$

The model parameters for quark and diquark distribution functions and their corresponding fragmentation functions have been mainly taken from the description of the data in [10, 11].

References

- [1] A. B. Kaidalov and K. A. Ter-Martirosyan, *Yad. Fiz.* **39**, 1545 (1984); **40**, 211 (1984).
- [2] A. Capella, U. Sukhatme, C. I. Tan, and J. Tran Thanh Van, *Phys. Rep.* **236**, 225 (1994);
A. Capella and J. Tran Thanh Van, *Z. Phys. C***10**, 249 (1981).
- [3] A. B. Kaidalov, K. A. Ter-Martirosyan, and Yu. M. Shabelski, *Yad. Fiz.* **43**, 1282 (1986).
- [4] Yu. M. Shabelski, *Yad. Fiz.* **44**, 186 (1986).
- [5] A. B. Kaidalov and O. I. Piskunova, *Yad. Fiz.* **41**, 1278 (1985).
- [6] Yu. M. Shabelski, *Yad. Fiz.* **49**, 1081 (1989).
- [7] V. A. Abramovski, V. N. Gribov, and O. V. Kancheli, *Yad. Fiz.* **18**, 595 (1973).
- [8] K. A. Ter-Martirosyan, *Phys. Lett. B***44**, 377(1973).
- [9] A. B. Kaidalov, *Sov. J. Nucl. Phys.* **45**, 902 (1987); *Yad. Fiz.* **43**, 1282 (1986).
- [10] G. H. Arakelyan, A. Capella, A. B. Kaidalov, and Yu. M. Shabelski, *Eur. Phys. J. C***26**, 81 (2002).
- [11] F. Bopp and Yu. M. Shabelski, *Yad. Fiz.* **68**, 2155 (2005); hep-ph/0406158 (2004).
- [12] F. Bopp and Yu. M. Shabelski, hep-ph/0603193 (2006).
- [13] G. H. Arakelyan, C. Merino, and Yu. M. Shabelski, *Yad. Fiz.* **69**, N.5 (2006) (in print); hep-ph/0505100 (2005).
- [14] X. Artru, *Nucl. Phys. B***85**, 442 (1975).
- [15] M. Imachi, S. Otsuki, and F. Toyoda, *Prog. Theor. Phys.* **54**, 280 (1976); **55**, 551 (1976).
- [16] G. C. Rossi and G. Veneziano, *Nucl. Phys. B***123**, 507 (1977).
- [17] H. Noda, *Progr. Theor. Phys.* **68**, 1406 (1982).
- [18] B. Z. Kopeliovich and B. G. Zakharov, *Z. Phys. C***43**, 241 (1989).
- [19] A. Capella, B. Z. Kopeliovich, *Phys. Lett. B***381**, 325 (1996).

- [20] D. Kharzeev, Phys. Lett. **B378**, 238 (1996).
- [21] B. Z. Kopeliovich and B. G. Zakharov, Phys. Lett. **B211**, 211 (1998);
E. Gotsman and S. Nusinov, Phys. Rev. **D22**, 624 (1980).
- [22] B. Z. Kopeliovich and B. Povh, Z. Phys. **C75**, 693, (1997).
- [23] A. Capella and C. A. Salgado, Phys. Rev. **C60**, 054906 (1999).
- [24] O. I. Piskounova, Proc. of the HERA-LHC Workshop, DESY, March 2005; Yad. Fiz. (in press).
- [25] P. R. S. Wright et al. (ABCCLVW Collaboration), Nucl. Phys. **B189**, 421 (1981).
- [26] M. Barth et al. (BCGMNS Collaboration), Z. Phys. **C10**, 213 (1981).
- [27] G. A. Alves et al. (E769 Collaboration), hep-ex/0303027; Phys. Lett. **B559**, 179 (2003).
- [28] E. A. De Wolf et al. (BCGMNS Collaboration), Nucl. Phys. **B246**, 431 (1984).
- [29] I. V. Ajinenko et al. (EHS-NA22 Collaboration), Z. Phys. **C44**, 573 (1989).
- [30] D. Brick et al., Nucl. Phys. **B164**, 1 (1980).
- [31] P. E. Volkovitsky, A. M. Lapidus, V. I. Lisin, and K. A. Ter-Martirosyan, Yad. Fiz. **24**, 1237 (1976).
- [32] A. E. Brenner et al., Phys. Rev. **D26** (1982) 1497.
- [33] H. Appelshauser et al. (NA49 Collaboration), Nucl. Phys. **A638**, 91c (1998).
- [34] V. V. Anisovich, M. N. Kobrinsky, J. Nyiri, and Yu. M. Shabelski, Usp. Fiz. Nauk **144**, 553 (1984); *Quark Model and High Energy Collisions*, World Scientific, Singapore (1985).